OPEN ACCESS



Constraints on Neutron Star Structure from the Clocked X-Ray Burster 1RXS J180408.9 -342058

A. Dohi (土肥明)^{1,2}, W. B. Iwakiri (岩切渉)³, N. Nishimura (西村信哉)^{1,4}, T. Noda (野田常雄)⁵, S. Nagataki (長瀧重博)^{1,2,6}, and M. Hashimoto (橋本正章)⁷

Astrophysical Big Bang Laboratory (ABBL), Cluster for Pioneering Research, RIKEN, Wako, Saitama 351-0198, Japan; akira.dohi@riken.jp
Interdisciplinary Theoretical and Mathematical Sciences Program (iTHEMS), RIKEN, Wako, Saitama 351-0198, Japan

³ International Center for Hadron Astrophysics, Chiba University, Chiba 263-8522, Japan

⁴ RIKEN Nishina Center for Accelerator-Based Science, Wako, Saitama 351-0198, Japan

⁷ Department of Physics, Kyushu University, Fukuoka 819-0395, Japan Received 2023 October 14; revised 2023 November 3; accepted 2023 November 4; published 2023 December 19

Abstract

Type I X-ray bursts are rapid-brightening transient phenomena on the surfaces of accreting neutron stars (NSs). Some X-ray bursts, called clocked bursters, exhibit regular behavior with similar light-curve profiles in their burst sequences. The periodic nature of clocked bursters has the advantage of constraining X-ray binary parameters and physics inside the NS. In the present study, we compute numerical models, based on different equations of state and NS masses, which are compared with the observations of a recently identified clocked burster, 1RXS J180408.9–342058. We find that the relation between the accretion rate and the recurrence time is highly sensitive to the NS mass and radius. We determine, in particular, that 1RXS J180408.9–342058 appears to possess a mass less than $1.7M_{\odot}$ and favors a stiffer nuclear equation of state (with an NS radius \gtrsim 12.7 km). Consequently, the observations of this new clocked burster may provide additional constraints for probing the structure of NSs.

Unified Astronomy Thesaurus concepts: X-ray bursts (1814); Neutron stars (1108); Low-mass x-ray binary stars (939)

1. Introduction

Type I X-ray bursts are rapidly evolving transient events observed from X-ray binaries, which are triggered by explosive thermonuclear burning on the accreting surface of a neutron star (NS). Observationally, 115 X-ray bursters have been identified (Galloway et al. 2020), and most of them show an irregular pattern in X-ray light curves. Some exceptional cases show that the recurrence time of a series of X-ray bursts is quite regular in a few sources, which are called clocked bursters. The most representative clocked burster is GS 1826–24 (see, e.g., Galloway et al. 2017 and references therein), which was first discovered in 1989 by the Ginga satellite (Tanaka 1989). Due to the regular properties of the light curves (e.g., the almost constant recurrence time Δt , peak luminosity, and burst duration), clocked bursters are helpful in probing the various physical properties of low-mass X-ray binaries (LMXBs) and in modeling X-ray bursts (e.g., Heger et al. 2007a; Meisel 2018; Johnston et al. 2020, for GS 1826–24). The observational light curves of GS 1826-24 also have been used for constraining relevant nuclear physics properties, such as the nuclear reaction rates involved in unstable proton-rich nuclei (Meisel et al. 2019; Hu et al. 2021; Lam et al. 2022a, 2022b) and the equation of state (EOS) and cooling of the central NS (Dohi et al. 2021, 2022).

Recent observations indicate that another X-ray burster, 1RXS J180408.9—342058 (hereafter, RX J1804), would show

Original content from this work may be used under the terms of the Creative Commons Attribution 4.0 licence. Any further distribution of this work must maintain attribution to the author(s) and the title of the work, journal citation and DOI.

the properties of a clocked burster. RX J1804 is an LMXB system found by the ROSAT satellite in 1990 (Voges et al. 1999), whose first X-ray burst event was detected by INTEGRAL in 2012 (Chenevez et al. 2012). In Wijnands et al. (2017) and Fiocchi et al. (2019), two epochs of X-ray bursts are observationally identified in hard and transitional X-ray states. As a distinctive feature, the observed recurrence time for each epoch is almost constant in each series of bursts, which may imply that RX J1804 may be a clocked burster.

In this work, we investigate the physical properties of NSs, e.g., the EoS, by modeling the newly observed clocked burster RX J1804. We use a general-relativistic stellar evolution code (the HERES code, described in Zhen et al. 2023) covering the whole NS regions. Such a numerical code enables us to investigate the NS physics, e.g., the EOS and neutrino cooling processes. For NS EOSs, there are many experimental and observational constraints (e.g., Sotani et al. 2022), but they still have large uncertainties. Our approach can constrain the NS EOS from astronomical observations through X-ray bursts.

The present paper is organized as follows. In Section 2, we summarize the observational properties of RX J1804 and the methods for our X-ray burst models. In Section 3, we present the results, compared with RX J1804 burst observations, and show the EOS and NS mass constraints. Section 4 is devoted to conclusions.

2. Methods

2.1. Observations of the Clocked Burster RX J1804

We present the method to constrain burst models from RX J1804 burst observations. First, we make numerical burst models with various \dot{M}_{-9} , in particular \dot{M}_{-9} – Δt relations,

Department of Education and Creation Engineering, Kurume Institute of Technology, Kurume, Fukuoka 830-0052, Japan Astrophysical Big Bang Group (ABBG), Okinawa Institute of Science and Technology Graduate University (OIST), Tancha, Onna-son, Kunigami-gun, Okinawa 904-0495, Japan

where \dot{M}_{-9} is the normalized accretion rate in units of $10^{-9}\,M_{\odot}\,\mathrm{yr}^{-1}$. Then we can obtain $\dot{M}_{-9,1\mathrm{st}}$ and $\dot{M}_{-9,2\mathrm{nd}}$ from each Δt , respectively. For the observational Δt and \dot{M}_{-9} of RX J1804, we take the results of Fiocchi et al. (2019), which analyzed the quasi-simultaneous INTEGRAL, SWIFT, and NuSTAR observational data over a very broad energy band of 0.8–200 keV. Namely, assuming the presence of the clocked X-ray bursters, the averaged Δt for each epoch is calculated as

$$\Delta t_{\rm 1st} = 2.20 \pm 0.04 \, \rm hr,$$
 (1)

$$\Delta t_{\rm 2nd} = 1.07 \pm 0.03 \,\text{hr},$$
 (2)

which determine $\dot{M}_{-9,1\text{st}}$ and $\dot{M}_{-9,2\text{nd}}$ for various burst models, respectively.

The other observation of RX J1804 is the *unabsorbed* persistent flux, which is given as follows (from Table 2 in Fiocchi et al. 2019):

$$f_{\text{per,1st}} = (45 \pm 13) \times 10^{-10} \,\text{erg cm}^{-2} \,\text{s}^{-1},$$
 (3)

$$f_{\text{per,2nd}} = (55 \pm 13) \times 10^{-10} \,\text{erg cm}^{-2} \,\text{s}^{-1},$$
 (4)

for the first and second epochs, respectively. Since the persistent flux is directly proportional to the accretion rate, we can deduce the observational ratio of accretion rates between different epochs as⁹

$$\frac{\dot{M}_{-9,2\text{nd}}}{\dot{M}_{-9,1\text{st}}} = 1.2 \pm 0.5. \tag{5}$$

Thus, we can judge the consistency of the model from $\dot{M}_{-9.2 \mathrm{nd}} / \dot{M}_{-9.1 \mathrm{st}}$ values.

A useful parameter to indicate the \dot{M}_{-9} - Δt relations is the η parameter, which is the power-law gradient being typically \sim 1, as (e.g., Lampe et al. 2016)

$$\Delta t \propto f_{\text{per}}^{-\eta} = k \dot{M}_{-9}^{-\eta},\tag{6}$$

where k is a constant. In fact, many burst observations show that the \dot{M}_{-9} - Δt relation matches with the power-law relationship with high accuracy. If $\eta=1$, there exists the critical mass of fuel for ignition $M_{\rm crit}\equiv \dot{M}_{-9}^{\eta}\Delta t$, but actually $\eta\neq 1$ from most observations, such as GS 1826-24 ($\eta=1.05\pm0.02$; Galloway et al. 2004) and MXB 1730-335 ($\eta=0.95\pm0.03$; Bagnoli et al. 2013). These facts imply that the amount of fuel for ignition varies with the accretion.

The η dependence of the model parameter has been investigated in detail by Lampe et al. (2016) with a 1D implicit hydrodynamics code with a large reaction network with up to 1300 nuclei, KEPLER (Woosley et al. 2004). Assuming the mass and radius of $M_{\rm NS}=1.4\,M_{\odot}$ and $R_{\rm NS}=11.2\,{\rm km}$, respectively, they calculated burst models with various $Z_{\rm CNO}$. They finally concluded that η varies from 1.1 to 1.24, but is weakly sensitive to $Z_{\rm CNO}$. However, their burst models seem to be incompatible with the recent burst observations of RX J1804; from the empirical relation of

Equation (6), one can get

$$\frac{\dot{M}_{-9,2\text{nd}}}{\dot{M}_{-9,1\text{st}}} = \left(\frac{\Delta t_{1\text{st}}}{\Delta t_{2\text{nd}}}\right)^{1/\eta} \simeq (2.05)^{1/\eta},\tag{7}$$

which results in $\eta \gtrsim 1.35$ for the case of Fiocchi et al. (2019). That is why we need to explore model parameters beyond Lampe et al. (2016) in order to explain the RX J1804 observations. As candidates, we pay attention to the NS mass and EOS, whose uncertainties highly affect Δt , due to the simultaneous change of surface gravitational and neutrino cooling effects (Dohi et al. 2021).

2.2. Multizone X-Ray Burst Models

To calculate X-ray burst models, we employ a multi-zone general-relativistic stellar evolution code, the HERES code, originally developed by Fujimoto et al. (1984); recent updates and a comparison to the MESA code are shown in Zhen et al. (2023). We follow the quasi-hydrostatic thermal evolution of bursting NSs through successive bursts with the nuclear burning of the approximated (88 nuclei) reaction network for mixed hydrogen and helium burning (Dohi et al. 2020). The HERES code consistently includes the central NS with the X-ray burst region, which allows us to investigate the dependency of the EOS on X-ray burst light curves (see, e.g., Dohi et al. 2021, 2022).

For the data of reaction rates, we mostly adopt the JINA Reaclib database ¹⁰ version 2.0 (Cyburt et al. 2010), except for the ⁶⁴Ge(p, γ)⁶⁵As and ⁶⁵As(p, γ)⁶⁶Se rates (Lam et al. 2016), which have significant impacts on light curves. Since we mostly focus on the impacts of the EOS on the recurrence time Δt as a representative burst output parameter, we adopt the above reaction set and do not change in the present study. Details of the numerical procedure of systematic X-ray burst calculations are the same as in Dohi et al. (2021). We describe the input parameters of our burst models.

As the NS microphysics, we employ three EOSs, i.e., Togashi (Togashi et al. 2017), LS220 (Lattimer & Swesty 1991), and TM1e (Shen et al. 2020), among which the radius is significantly different (see Figure 1 in Dohi et al. 2021); there still remain uncertainties in the NS radius, which is $R_{\rm NS} \sim 11$ –14 km with $1.4\,M_{\odot}$. The treatment of heating and cooling processes inside NSs is the same as in Dohi et al. (2021), in which the conventional crustal heating process and the slow ν -cooling process, mainly composed of the modified Urca process and Bremsstrahlung, ¹¹ are implemented. The fast cooling processes, such as the direct Urca process, could occur and have impacts on the X-ray bursts in heavy NSs (and EOSs with large symmetry energy; Dohi et al. 2022), but for simplicity we ignore this effect in the present study.

The observed light curves of RX J1804 show that these X-ray bursts are triggered by mixed H/He burning (Wijnands et al. 2017; Fiocchi et al. 2019), implying $\dot{M}_{-9} \gtrsim 1$ due to the stability conditions of nuclear burning (Fujimoto et al. 1981; Bildsten 1998). We accordingly choose $\dot{M}_{-9} = 2$ –9. Another crucial input parameter is the composition of accreted matter, in particular for the metallicity $Z_{\rm CNO}$. As RX J1804 locates in the

⁸ We average the values of the peak time $(T_{\rm peak})$ for each burst, which are listed in Table 3 of Fiocchi et al. (2019).

⁹ Note that the best-fit column density obtained from spectral fitting is the same between two phases (Fiocchi et al. 2019), so the ratio of accretion rate ratios can be simply obtained as the ratio between Equations (3) and (4).

¹⁰ https://reaclib.jinaweb.org

¹¹ The enhanced cooling by nucleon superfluidity can be ignored, since the core temperature is much lower than the transition temperature (Dohi et al. 2022).

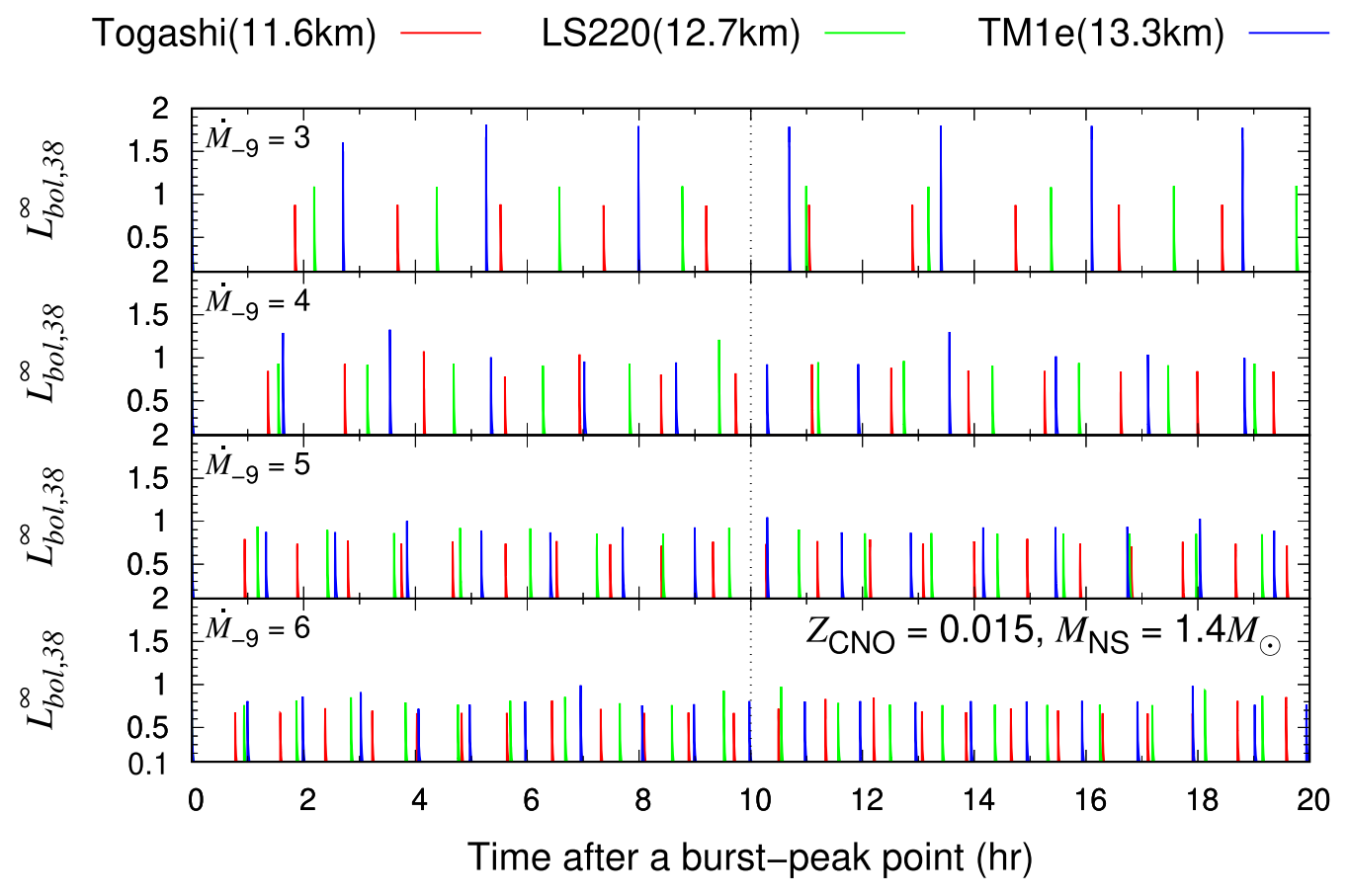


Figure 1. EOS dependence of averaged light curves during 20 hr with $1.4M_{\odot}$ NSs and $Z_{\rm CNO} = 0.015$. The horizontal axis indicates the time where a time at the peak point is set to be zero, and the vertical axis indicates the bolometric luminosity in units of 10^{38} erg s⁻¹. $\dot{M}_{-9} = 3$ (top), $\dot{M}_{-9} = 4$ (second top), $\dot{M}_{-9} = 5$ (second bottom), and $\dot{M}_{-9} = 6$ (bottom).

global cluster in the Galactic bulge (Voges et al. 1999), which implies relatively higher metallicity, we choose $Z_{\rm CNO} = 0.01$, 0.015, and 0.02, including ¹⁴O and ¹⁵O at a ratio of 7 to 13. For the mass fraction of light elements, we fix to the solar abundance ratio, X/Y = 2.9.

3. Results

Figure 1 shows X-ray burst light curves with various mass accretion rates and different EOSs. As shown by Dohi et al. (2021), a large-radius (stiff) EOS has a high Δt and high peak luminosity for all mass accretion rates. This is because of the lower surface gravity, which requires a greater amount of fuel for the ignition. Although the Δt significantly depends on the mass accretion rates, where higher M_{-9} shows a shorter Δt , we clearly find the above EOS dependence.

The averaged Δt values with different EOSs and \dot{M}_{-9} are presented in Figure 2. We can see that a stiffer EOS generally results in a higher Δt , except for the case of the lowest $\dot{M}_{-9} = 2$. Interestingly, in these low- \dot{M} models, the dependence on the stiffness of the EOS becomes reversed. This phenomenon occurs due to the proximity of the peak luminosity to the Eddington luminosity at low \dot{M} . Consequently, the compressional heating luminosity caused by the gravitational release of NSs becomes more influential, and the effect of surface gravity becomes relatively more significant (see also Zhen et al. 2023).

By applying the fitting formula given by Equation (6) to the $\Delta t - \dot{M}_{-9}$ relations, as shown in Figure 2, we obtain the

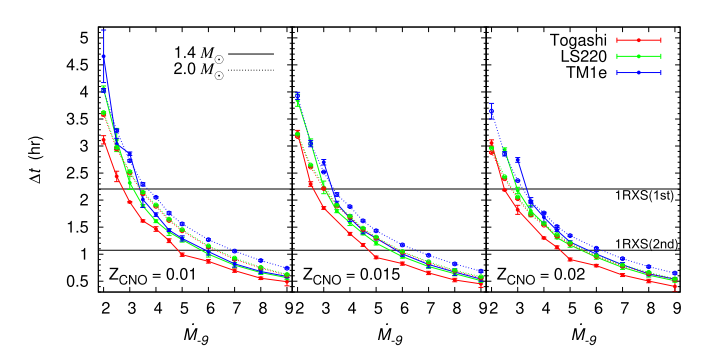


Figure 2. EOS dependence of averaged Δt with 1σ errors. The solid curves indicate 1.4 M_{\odot} NSs, while the dotted curves indicate 2 M_{\odot} NSs. The metallicity $Z_{\rm CNO}$ is chosen to be 0.01 (left), 0.015 (middle), and 0.02 (right). The observational Δt of RX J1804 for the first and second epochs are plotted.

corresponding η values shown in Figure 3. We note that the η and k values lie within less than 10% error for all parameter regions of $Z_{\rm CNO}$, the EOS, and the NS mass. We find that stiffer EOSs tend to have higher η values, due to their lower Δt values. Additionally, lower-mass models exhibit higher η values. Remarkably, η strongly reflects the stiffness of the EOS, unlike the Δt value, which is also influenced by ν -cooling effects. Therefore, η could be a powerful indicator for constraining the NS structure.

In the previous works (Lampe et al. 2016), the η values lie in the range of 1.1–1.24, assuming $M_{\rm NS}=1.4\,M_{\odot}$ and $R_{\rm NS}=11.2\,{\rm km}$, but we find that the original finding range

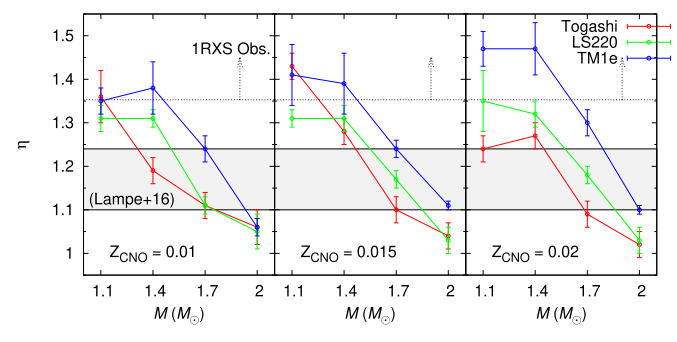


Figure 3. η values as a function of NS masses. We also show the range obtained from previous works (Lampe et al. 2016) and the lower limit of RX J1804 implied from Equation (7).

can be extended if the mass and radius are changed. The closest models to Lampe et al. (2016) for model parameters are those with $M_{\rm NS}=1.4\,M_{\odot}$ and the Togashi EOS ($R_{\rm NS}=11.6\,{\rm km}$). In such NSs, η values with $Z_{\rm CNO}=0.015$ and 0.02 are slightly higher than the range expected previously, though those with $Z_{\rm CNO}=0.01$ are consistent. However, since the influence of EOS uncertainties on η is large, as in Figure 3, the difference in radius between 11.2 and 11.6 km may not be small. Moreover, we can confirm that the metallicity dependence on η is not so large as found in Lampe et al. (2016). Thus, these facts imply that our burst models are qualitatively consistent with Lampe et al. (2016).

Except for Δt , the other observational factor for RX J1804 is the ratio of persistent flux between both epochs, i.e., the accretion rate ratio. To clarify the connection between η and the accretion rate ratio, we show a schematic picture in Figure 4. First, we can find the crosspoints $(\dot{M}_{-9,1\text{st}}$ and $\dot{M}_{-9,2\text{nd}})$ between theoretical curves and RX J1804 observations for the first and second epochs, respectively. Then, since $\eta > 1$ and $\dot{M}_{-9} \gtrsim 1$ for RX J1804, η should be higher if the difference between crosspoints for the first and second epochs, i.e., $\dot{M}_{-9,2\text{nd}}/\dot{M}_{-9,1\text{st}}-1$, becomes smaller. Thus, the accretion rate should have a negative correlation with η .

Thus, we finally obtain the accretion rate ratio as shown in Figure 5. 12 If the NS is more compact, the accretion rate ratio tends to be higher, as we explain above. By comparing the observational constraint for RX J1804, i.e., Equation (5), one can see that RX J1804 should be light, with at least $M_{\rm NS} < 1.7\,M_{\odot}$. This result may be peculiar in LMXBs because typical accreting NSs always get their mass from the companion over a long timescale (~Gyr) and finally tend to become heavy. In fact, most observations show that accreting NSs in LMXBs are heavy (Özel & Freire 2016; Alsing et al. 2018; see also Romani et al. 2022). Our results thus imply that RX J1804, born just after the supernova explosion, might be a very light NS. However, this may be against the standard supernova explosion theory (Suwa et al. 2018; but see also Doroshenko et al. 2022 for recent observations). Thus, our study brings up the issue of how such low-mass NSs are born.

Regarding the EOS dependence, the small-radius models tend to have lower $\dot{M}_{-9,2{\rm nd}}/\dot{M}_{-9,1{\rm st}}-1$. In the case of $M_{\rm NS}=1.4\,M_{\odot}$, only the Togashi EOS is inconsistent with RX J1804 observations, regardless of the metallicity. This

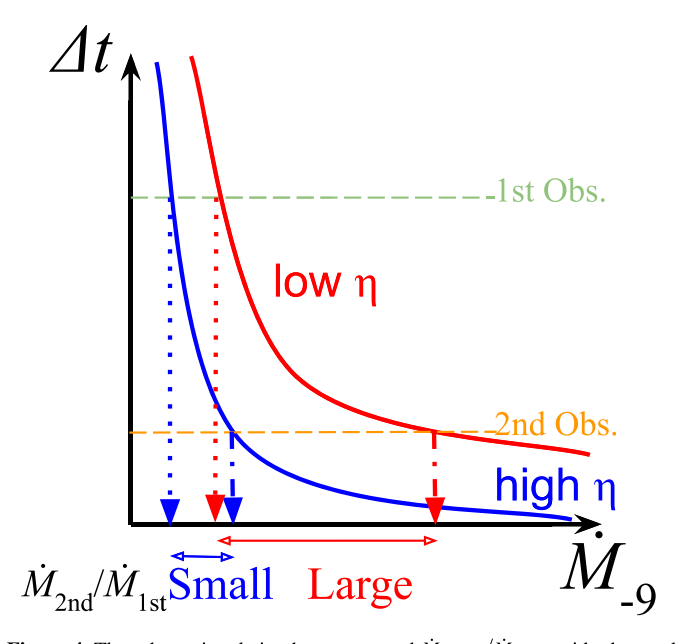


Figure 4. The schematic relation between η and $\dot{M}_{-9,2{\rm nd}}/\dot{M}_{-9,1{\rm st}}$ with observed $\Delta t_{1{\rm st}}$ and $\Delta t_{2{\rm nd}}$ for RX J1804.

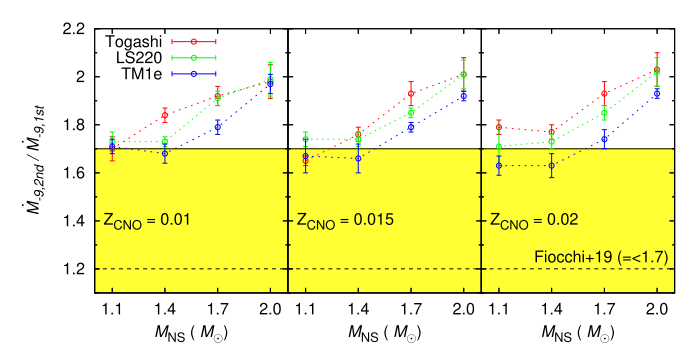


Figure 5. The same as Figure 2, but for the accretion rate ratio between the first and second epochs. The observational constraint for RX J1804, Equation (5), is also plotted.

implies a larger radius with $1.4\,M_\odot$ NSs than 12.7 km, corresponding to that with the LS220 EOS. A similar constraint can be obtained for $1.1\,M_\odot$ NSs, but it becomes laxer compared with $1.4\,M_\odot$ NSs. Thus, we suggest that the observational accretion rate ratio is a new and powerful tool to constrain the NS structure.

4. Conclusions

We performed numerical calculations to model a newly discovered clocked burster RX J1804 for the first time. From the observed recurrence time and persistent flux in two epochs, we found that RX J1804 could become a powerful site to constrain EOSs, even without light-curve modeling. Specifically, small-radius EOSs such as the Togashi are disfavored. This trend is against that of the clocked burster GS 1826–24, where large-radius EOSs ($R_{\rm NS} \gtrsim 14$ km) are disfavored due to the photospheric radius expansion (Dohi et al. 2021; but see also Johnston et al. 2020). Thus, the combination of GS 1826–24 and RX J1804 gives tight constraints on EOSs, i.e., $R_{\rm NS} \sim 13$ km in the case of $1.4\,M_{\odot}$ NSs.

In our burst models, we considered the *standard* energy sources inside accreting NSs, but additional sources may

 $[\]overline{12}$ Our calculation fixes the global accretion rate, which means that the local accretion rate per unit area $\frac{M}{4\pi R_{NS}^2}$ varies with the EOS and mass. However, since the accretion rate ratio is the same as both the global and the local accretion rate, our conclusion holds.

change our results. The one of the sources is a shallow heating process inferred from observations (e.g., Deibel et al. 2015), though the physical origin is unknown. For the RX J1804 burster, some studies indicate the existence of a shallow heating source with \sim 0.9 MeV per accreted nucleon during the outburst state (Parikh et al. 2017, 2018). The increase of the deep crustal heating rate by \sim 0.9 MeV u⁻¹ could highly decrease Δt , depending on the model parameters (Meisel 2018). This may reduce the slope in the \dot{M}_{-9} – Δt plane, i.e., η , leading to a higher accretion rate ratio. The present constraints on EOSs are therefore *minimal* ones, which must be more rigid in the presence of shallow heating.

Not only the heating but also the cooling processes may be open, such as the strong neutrino Urca cycle in the inner crust (Schatz et al. 2014) and the direct Urca process in the core. A wider investigation of the present model parameters regarding the energy sources is therefore needed and left for our future work. Nevertheless, we emphasize that energy sources in the crust must be there in all accreting NSs, and the differences of Δt among mass/radius might not be so large. Furthermore, the direct Urca process (or more exotic ν -cooling processes) is unlikely to occur, according to our conclusion that stiffer NSs, i.e., with a lower central density, are favored in RX J1804. In these senses, even if the additional energy sources are considered, our conclusion should qualitatively hold.

In this work, we only compared Δt and the accretion rate ratio, but the shapes of light curves are needless to say important to constrain the model parameters above all for reaction rates, whose uncertainties are reflected in the tail parts (e.g., Meisel et al. 2019). The burst duration, the time from the peak luminosity to the half of peak one, is found to be about 30-40 s for RX J1804 (Fiocchi et al. 2019), which is similar to (or a little shorter than) GS 1826-24. This must imply high metallicity, according to Heger et al. (2007a) and Lampe et al. (2016). ¹⁴ Moreover, such a long tail of the light curve may suggest that the rapid proton capture process is very active to synthesize very heavy proton-rich nuclei with the mass number ~ 100 (Schatz et al. 2001). Thus, since the accretion rate is quite high, in particular for the first epoch, a millihertz quasiperiodic oscillation, which is triggered by marginal stable nuclear burning (Heger et al. 2007b; Keek et al. 2014; Liu et al. 2023), could occur in RX J1804, and actually has been detected by XMM-Newton observations (Tse et al. 2021). Thus, the burst light curves of RX J1804 have many interesting features and must provide much helpful information on nuclear astrophysics. Future work is expected to analyze the burst profiles of RX J1804, to produce observational light curves comparable with our burst models. We will present the constraints on various model parameters by fitting the light curves of RX J1804 elsewhere.

Acknowledgments

We thank T. Tamagawa for giving useful comments. A.D. also thanks E. Britt, E. Brown, R. Jain, and H. Schatz for fruitful discussion and warm hospitality during his stay at the

FRIB. A.D. and N.N. were financially supported by IReNA (International Research Network for Nuclear Astrophysics). This project was financially supported by JSPS KAKENHI (19H00693, 20H05648, 21H01087, and 23K19056), the RIKEN Pioneering Project "Evolution of Matter in the Universe" (r-EMU), and the RIKEN Incentive Research Project. Parts of the computations were carried out on computer facilities at CfCA in NAOJ and at YITP, Kyoto University.

ORCID iDs

```
References
Alsing, J., Silva, H. O., & Berti, E. 2018, MNRAS, 478, 1377
Bagnoli, T., in't Zand, J. J. M., Galloway, D. K., & Watts, A. L. 2013,
         AS 431 1947
Bildsten, L. 1998, in The Many Faces of Neutron Stars, ed. R. Buccheri,
   J. van Paradijs, & A. Alpar (Dordrecht: Kluwer), 419
Brown, E. F., 2015 dStar: Neutron Star Thermal Evolution Code, Astrophysics
   Source Code Library, ascl:1505.034
Chenevez, J., Kuulkers, E., Brandt, S., et al. 2012, ATel, 4050
Cyburt, R. H., Amthor, A. M., Ferguson, R., et al. 2010, ApJS, 189, 240
Deibel, A., Cumming, A., Brown, E. F., & Page, D. 2015, ApJL, 809, L31
Dohi, A., Hashimoto, M.-a., Yamada, R., Matsuo, Y., & Fujimoto, M. Y. 2020,
    TEP, 2020, 033E02
Dohi, A., Nishimura, N., Hashimoto, M., et al. 2021, ApJ, 923, 64
Dohi, A., Nishimura, N., Sotani, H., et al. 2022, ApJ, 937, 124
Doroshenko, V., Suleimanov, V., Pühlhofer, G., & Santangelo, A. 2022,
   NatAs, 6, 1444
Fiocchi, M., Bazzano, A., Bruni, G., et al. 2019, ApJ, 887, 30
Fujimoto, M. Y., Hanawa, T., Iben, I., Jr., & Richardson, M. B. 1984, ApJ,
Fujimoto, M. Y., Hanawa, T., & Miyaji, S. 1981, ApJ, 247, 267
Galloway, D. K., Cumming, A., Kuulkers, E., et al. 2004, ApJ, 601, 466
Galloway, D. K., Goodwin, A. J., & Keek, L. 2017, PASA, 34, e019
Galloway, D. K., in't Zand, J., Chenevez, J., et al. 2020, ApJS, 249, 32
Heger, A., Cumming, A., Galloway, D. K., & Woosley, S. E. 2007a, ApJL,
   671, L141
Heger, A., Cumming, A., & Woosley, S. E. 2007b, ApJ, 665, 1311
Hu, J., Yamaguchi, H., Lam, Y. H., et al. 2021, PhRvL, 127, 172701
Johnston, Z., Heger, A., & Galloway, D. K. 2020, MNRAS, 494, 4576
Keek, L., Cyburt, R. H., & Heger, A. 2014, ApJ, 787, 101
Lam, Y. H., He, J. J., Parikh, A., et al. 2016, ApJ, 818, 78
Lam, Y. H., Liu, Z. X., Heger, A., et al. 2022a, ApJ, 929, 72
Lam, Y. H., Lu, N., Heger, A., et al. 2022b, ApJ, 929, 73
Lampe, N., Heger, A., & Galloway, D. K. 2016, ApJ, 819, 46
Lattimer, J. M., & Swesty, D. F. 1991, NuPhA, 535, 331
Liu, H., Gao, Y., Li, Z., et al. 2023, MNRAS, 525, 2054
Meisel, Z. 2018, ApJ, 860, 147
Meisel, Z., Merz, G., & Medvid, S. 2019, ApJ, 872, 84
Özel, F., & Freire, P. 2016, ARA&A, 54, 401
Page, D., & Reddy, S. 2013, PhRvL, 111, 241102
Parikh, A. S., Wijnands, R., Degenaar, N., et al. 2017, MNRAS, 466, 4074
Parikh, A. S., Wijnands, R., Degenaar, N., Ootes, L., & Page, D. 2018,
     NRAS, 476, 2230
Romani, R. W., Kandel, D., Filippenko, A. V., Brink, T. G., & Zheng, W.
   2022, ApJL, 934, L17
```

Schatz, H., Aprahamian, A., Barnard, V., et al. 2001, PhRvL, 86, 3471

Schatz, H., Gupta, S., Möller, P., et al. 2014, Natur, 505, 62

Shen, H., Ji, F., Hu, J., & Sumiyoshi, K. 2020, ApJ, 891, 148 Sotani, H., Nishimura, N., & Naito, T. 2022, PTEP, 2022, 041D01

 $[\]overline{^{13}}$ This result is obtained with use of the NSCOOL code modified for accreting NSs (Page & Reddy 2013), which was also confirmed to be well reproduced with the dSTAR code developed by Brown (2015; R. Jain 2023, private communication).

 $^{^{14}}$ In fact, assuming that the count rate to flux conversion factor is independent of energy, our models also indicate $Z_{\rm CNO} \simeq 2\%$ from the observed burst duration.

Suwa, Y., Yoshida, T., Shibata, M., Umeda, H., & Takahashi, K. 2018, MNRAS, 481, 3305

Tanaka, Y. 1989, in Proc. of the 23rd ESLAB Symposium on Two Topics in X-Ray Astronomy, ed. J. Hunt & B. Battrick (Paris: ESA), 3 Togashi, H., Nakazato, K., Takehara, Y., et al. 2017, NuPhA, 961, 78

Tse, K., Galloway, D. K., Chou, Y., Heger, A., & Hsieh, H.-E. 2021, MNRAS,

500, 34

Voges, W., Aschenbach, B., Boller, T., et al. 1999, A&A, 349, 389 Wijnands, R., Parikh, A. S., Altamirano, D., Homan, J., & Degenaar, N. 2017, MNRAS, 472, 559

Woosley, S. E., Heger, A., Cumming, A., et al. 2004, ApJS, 151, 75 Zhen, G., Lü, G., Liu, H., et al. 2023, ApJ, 950, 110